Josephson-Junction Qubits

Yuriy Makhlin*,†, Gerd Schön*,‡, and Alexander Shnirman*
*Institut für Theoretische Festkörperphysik, Universität Karlsruhe, D-76128 Karlsruhe, Germany
†Landau Institute for Theoretical Physics, Kosygin St. 2, 117940 Moscow, Russia
‡Forschungszentrum Karlsruhe, Institut für Nanotechnologie, D-76021 Karlsruhe, Germany

Among the potential physical implementations of quantum bits (qubits) solid state devices appear most promising for large scale applications and integration in electronic circuits. Devices based on low-capacitance Josephson junctions exploit the coherence of the superconducting state, combined with the possibility to control individual charges by Coulomb blockade effects. The logical states in these systems differ by one Cooper-pair charge. Single- and two-bit operations can be performed by applying a sequence of gate voltages. The phase coherence time is sufficiently long to allow a series of these steps. If, in addition, the strength of the Josephson coupling is controlled (e.g. by currents in SQUID loops) the system is ideal for quantum computation. Recent experiments by Nakamura *et al.* show the feasibility of this approach.

In addition to the manipulations of qubits the resulting quantum state has to be read out. This quantum measurement process can be accomplished by coupling a single-electron transistor (SET) capacitively to the qubit. We investigate the process by analyzing the time-evolution of the density matrix of the coupled system. The measurement process is characterized by three time scales: the dephasing time, which is fast when a dissipative current flows in the SET, a longer 'measurement time' needed to read out the signal, and a third, even longer 'mixing time', characterizing measurement induced transitions which destroy the information about the initial quantum state. The noise spectrum of the current in the SET displays these time scales and allows their direct observation.

Quantum computers, if available, could perform certain operations in a massive parallel way, which would lead to an exponential speed-up as compared to the performance of classical computers. Medium-size quantum information processing devices could be used in a number of applications such as, e.g., quantum communication and quantum cryptography. Several physical realizations of quantum bits, the elementary building blocks of quantum computers, have been proposed. Best studied are trapped ions, NMR in the liquid state and cavity QED. Here we discuss solid-state nano-electronic realizations. They appear most promising since they can be scaled up to large numbers of qubits and are most easily embedded in electronic circuits.

Josephson junction circuits are particularly suitable for quantum information processing, since they combine the intrinsic coherence of the superconducting state and the possibility to control the circuit dynamics by voltage and magnetic flux pulses. Their fabrication and manipulation are possible by present-day technologies. The relevant dynamical variables in these circuits are the charges on the islands and the phases of the superconducting order parameter. Both are canonically conjugated, with Heisenberg's uncertainty principle holding for them. Depending on the ratio of two characteristic energies – the typical charging energy, which favors well-defined charges, and the Josephson energy, which favors sharp values of the phase degree of freedom – the charge or the flux form a good basis, while the other fluctuates strongly. Either charge [1–3] or phase [4,5] degrees of freedom can be used to store and process quantum information. Encouraged by successful earlier experiments which demonstrated that superpositions of charge states exist [6–8], as well as by recent experiments which demonstrated quantum coherent oscillations of a superposition of eigenstates [9] we consider here low-capacitance Josephson junctions in the charge regime.

The plan of the paper is as follows. First, we introduce an ideal model for a quantum register and analyze how various steps of quantum computation are performed. Then we discuss the simple design of a qubit proposed in Ref. [1] as well as an improved design with controlled Josephson couplings proposed in Ref. [2]. We analyze the inter-qubit coupling via a high frequency oscillator mode [1,2] and show that the improved qubit design is close to ideal. Finally we describe the read-out, i.e., the quantum measurement of the state of a qubit [10–12].

A quantum computer may be realized, for example, by a system with the following model Hamiltonian

$$H = -\sum_{i=1}^{N} \left[E_z^i(t)\hat{\sigma}_z^i + E_x^i(t)\hat{\sigma}_x^i\right] + \sum_{i\neq j} A^{ij}(t)\hat{\sigma}_+^i\hat{\sigma}_-^j \ . \quad (1)$$

A spin notation is used for the qubits with Pauli matrices $\hat{\sigma}_z$, $\hat{\sigma}_x$, $\hat{\sigma}_\pm = \frac{1}{2}(\hat{\sigma}_x \pm i\hat{\sigma}_y)$. Ideally, each energy $E_z^i(t)$, $E_x^i(t)$ and the (real symmetric) couplings $A^{ij}(t)$ can be switched separately for controlled times between zero and finite values, E_z^i, E_x^i and A^{ij}. We assume that E_z^i is the largest energy, suggesting the choice of basis states $|\uparrow_i\rangle$ and $|\downarrow_i\rangle$ aligned along the z-axis. Residual inelastic interactions, which destroy the coherence, and the measurement device, when turned on, should be accounted for by extra terms $H_{\rm res}$ and $H_{\rm meas}(t)$, respectively.
(i) To prepare this system in a well defined initial state

we turn on at low temperature large values of $E_z^i \gg k_{\rm B}T$ for all i (while $E_x^i(t) = A^{ij}(t) = 0$). After sufficient time the residual interaction $H_{\rm res}$ has relaxed all spins to the ground state, $|\uparrow\uparrow\uparrow ...\rangle$. Then we set $E_z^i(t)$ back to zero.
(ii) Single-bit operations are controlled by turning on one of the $E_x^i(t)$. Then spin i evolves according to the unitary transformation

$$U_x(\alpha) = \exp(iE_x^i\tau\hat{\sigma}_x^i/\hbar) = \begin{pmatrix} \cos\alpha & i\sin\alpha \\ i\sin\alpha & \cos\alpha \end{pmatrix} , \qquad (2)$$

where $\alpha = E_x^i\tau/\hbar$. Depending on the time span τ, a π- or $\pi/2$-rotation can be performed, producing a spin flip or an equal-weight superposition of spin states. Switching on $E_z^i(t)$ produces another needed operation: a phase shift between $|\uparrow_i\rangle$ and $|\downarrow_i\rangle$. Back in the idle state, where $H = 0$, the relative phase shift of the states does not evolve further.
(iii) A two-bit operation on qubits i and j is achieved by turning on the corresponding $A^{ij}(t)$. In the basis $|\uparrow_i\uparrow_j\rangle$, $|\uparrow_i\downarrow_j\rangle$, $|\downarrow_i\uparrow_j\rangle$, $|\downarrow_i\downarrow_j\rangle$ the result is described by

$$U_{2\rm b}^{ij}(\tau) = \begin{pmatrix} 1 & 0 & 0 & 0 \\ 0 & \cos\beta & i\sin\beta & 0 \\ 0 & i\sin\beta & \cos\beta & 0 \\ 0 & 0 & 0 & 1 \end{pmatrix} , \qquad (3)$$

with $\beta = A^{ij}\tau/\hbar$. For $\beta = \pi/2$ the result is a spin-swap operation, while $\beta = \pi/4$ yields a 'square-root of swap', which transforms the state $|\uparrow_i\downarrow_j\rangle$ into the entangled state $\frac{1}{\sqrt{2}}\left(|\uparrow_i\downarrow_j\rangle + i\,|\downarrow_i\uparrow_j\rangle\right)$. This operation, in combination with single-bit operations, allows us to perform the 'controlled-not' gate. Moreover, the 'square-root of swap' gate together with the one-bit operations provide a universal set, sufficient for all logic gates of quantum computations [13].
(iv) The measurement process will be discussed for specific realizations (see below).

The simplest example of the Josephson qubit proposed in Ref. [1] is the superconducting electron (Cooper pair) box shown in Fig. 1a). It consists of a superconducting island connected by a Josephson junction to a superconducting lead and via a gate capacitor C to another lead. A control voltage $V_{\rm x}$ is applied via the gate capacitor. The Josephson junction is characterized by the Josephson energy $E_{\rm J}$ (which is related to the Josephson critical current $I_{\rm c}$ by $E_{\rm J} = I_{\rm c}\Phi_0/2\pi$, and $\Phi_0 \equiv h/2e$ is the flux quantum) and by the capacitance $C_{\rm J}$ which determines the charging energy scale. The relevant conjugate variables are the phase difference Θ across the junction and the charge $Q = 2ne$ on the island (n being the number of Cooper pairs). If normal electron (quasiparticle) tunneling is suppressed by the superconducting energy gap and only 'even-parity' states are involved [14], the circuit dynamics is described by the Hamiltonian

$$H = \frac{(Q - CV_{\rm x})^2}{2(C + C_{\rm J})} - E_{\rm J}\cos\left(2\pi\frac{\Theta}{\Phi_0}\right) \quad ; \quad Q = \frac{\hbar}{i}\frac{\partial}{\partial\Theta}. \qquad (4)$$

Here we consider junctions where the charging energy with scale $E_C \equiv e^2/2(C+C_{\rm J})$ dominates over the Josephson coupling $E_{\rm J}$. It is plotted in Fig. 2 as a function of the external voltage $V_{\rm x}$ for different n. In equilibrium at $k_{\rm B}T \ll E_C$, the system is in the state corresponding to the lowest parabola. However, near the voltages $V_{\rm deg} = (2n+1)e/C$ the states n and $n+1$ are near-degenerate, and even a weak $E_{\rm J}$ mixes them strongly. Here, in the basis of charge states $|\downarrow\rangle = |n\rangle$ and $|\uparrow\rangle = |n+1\rangle$, the Hamiltonian reduces to a two-state model

$$H = E_{\rm ch}(V_{\rm x})\hat{\sigma}_z - \frac{1}{2}E_{\rm J}\hat{\sigma}_x , \qquad (5)$$

where $E_{\rm ch}(V_{\rm x}) = e(V_{\rm x} - V_{\rm deg})C_{\rm qb}/C_{\rm J}$, and the capacitance of the qubit in the circuit is $C_{\rm qb}^{-1} = C_{\rm J}^{-1} + C^{-1}$.

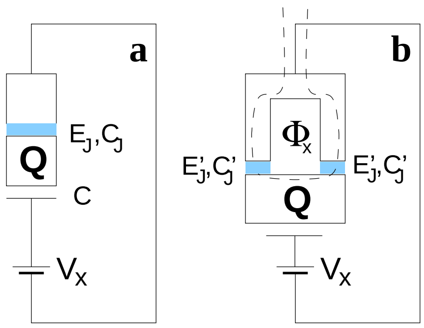

FIG. 1. **Josephson junction qubits.** a) A simple realization of a qubit is provided by the superconducting electron box. The important degree of freedom is the Cooper pair charge $Q = 2en$ on the island between gate capacitor C and Josephson junction (grey area) with capacitance $C_{\rm J}$ and Josephson coupling energy $E_{\rm J}$.
b) The improved design of the qubit. The island is coupled to the circuit via two Josephson junctions with parameters $C'_{\rm J}$ and $E'_{\rm J}$. This dc-SQUID can be tuned by the external flux which is controlled by the current through the inductor loop (dashed line). The setup allows switching the effective Josephson coupling to zero.

On the way towards the ideal model (1) we achieved a tunable $E_z^i(t)$, however, the Josephson coupling is fixed $E_x^i(t) = E_{\rm J}/2$. Still single-bit operations can be performed [1] by controlling the bias voltage $V_{\rm x}$, as it was experimentally demonstrated by Nakamura et al. [9]. In this experiment the system is prepared in the state $|\downarrow_i\rangle$ by setting the gate voltage such that $E_z^i(t) \gg E_x^i, k_{\rm B}T$ and waiting long enough for the relaxation to the ground state to occur. Then (ideally) one switches the gate voltage suddenly to the degeneracy point $E_z^i(t) = 0$, where the system is kept for a time Δt. The remaining part of the Hamiltonian $E_x^i\sigma_x$ produces coherent oscillations described by the unitary transformation $\exp(iE_x^i\Delta t\hat{\sigma}_x^i/\hbar)$. Finally the resulting state is "frozen" by switching back to the regime $E_z^i(t) \gg E_x^i$. In the experiment the current across an extra junction was measured, which probes the probability for the system to end up in the excited state. This signal showed – time resolved – the coherent oscillations with the expected frequency $E_x^i \Delta t/\hbar$. It is the first successful experiment of this kind with a controlled fabricated electronic device.

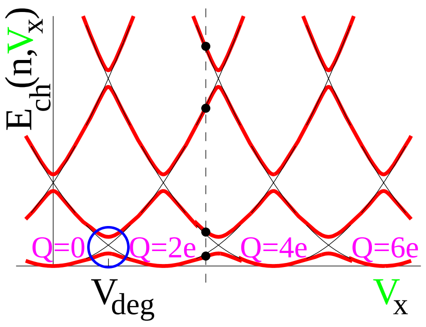

FIG. 2. **Spectrum of a superconducting electron box.** The charging energy of the superconducting electron box is shown (solid lines) as a function of the applied gate voltage V_x for different numbers n of extra Cooper pairs on the island. Near degeneracy points the weaker Josephson coupling energy mixes the charge states and modifies the energy of the eigenstates (dotted line). In this regime the system effectively reduces to a 2-state quantum system.

A crucial step towards the ideal model (1) is to make the Josephson coupling tunable. On one hand, this allows us to really freeze the state of the qubit completely by switching to $H = 0$. Unless this is done, the continuing time evolution of the phases of the states has to be taken into account carefully in successive gate operations. On the other hand, as we will discuss below, the tunable Josephson coupling also allows us to switch the two-bit coupling off and on. The Josephson coupling can be tuned in the design of Fig. 1b), where the Josephson junction is replaced by a dc-SQUID biased by an external flux Φ_x. The dc-SQUID is a superconducting loop cut by two, ideally identical, Josephson junctions. One half of the loop serves as the qubit's island, while the other half is the superconducting lead. The controllable external flux is coupled into the system through an inductor loop. The system is described by the two phase drops Φ_1 and Φ_2 across two Josephson junctions. The natural degrees of freedom are the total flux in the SQUID $\Phi \equiv \Phi_1 - \Phi_2$ and the average phase drop $\Theta \equiv (\Phi_1 + \Phi_2)/2$. If the SQUID's self-inductance L_Φ is low, $\Phi_0^2/L_\Phi \gg 4\pi^2 E_\mathrm{J}', e^2/C_\mathrm{J}'$, the total magnetic flux in the SQUID Φ fluctuates weakly around Φ_x, $\sqrt{\langle(\Phi - \Phi_\mathrm{x})^2\rangle} \ll \Phi_0$. Furthermore, if the frequency of flux oscillations is high, $\hbar\omega_\Phi = \hbar(L_\Phi C_\mathrm{J}'/2)^{-1/2} \gg E_\mathrm{J}'$, E_ch, $k_\mathrm{B}T$, the Φ-degree of freedom is in the ground state. In this case one can neglect the quantum fluctuations of Φ, assume $\Phi = \Phi_x$, and describe the SQUID-controlled qubit by a Hamiltonian of the form (4), with Josephson term

$$\begin{aligned} &E_\mathrm{J}' \cos(2\pi\Phi_1/\Phi_0) + E_\mathrm{J}' \cos(2\pi\Phi_2/\Phi_0) \\ &= 2E_\mathrm{J}' \cos(\pi\Phi_\mathrm{x}/\Phi_0)\cos(2\pi\Theta/\Phi_0) \end{aligned} \tag{6}$$

and effective junction capacitance $C_\mathrm{J} = 2C_\mathrm{J}'$. I.e., the effective Josephson coupling

$$E_\mathrm{J}(\Phi_\mathrm{x}) = 2E_\mathrm{J}' \cos(\pi\Phi_\mathrm{x}/\Phi_0) \tag{7}$$

is tunable by the external flux Φ_x between $2E_\mathrm{J}'$ and zero. (Clearly, $E_\mathrm{J} = 0$ requires the Josephson energies of two junctions in the loop to be equal. This has been reached with a precision of 1% in quantum tunneling experiments [15], introducing relatively small computational errors. Alternatively, by replacing the SQUID by a 3-junction geometry, one can tune the effective Josephson couplings exactly to zero.)

Thus, the SQUID-controlled qubit is compatible with the ideal model (1) on the one-bit level. The energies E_z^i and E_x^i are controlled independently by the gate voltage and the external flux. In the idle state we keep $V_\mathrm{x} = V_\mathrm{deg}$ and $\Phi_\mathrm{x} = \Phi_0/2$ so that the Hamiltonian $H = 0$. Changing one of them generates rotations around z- or x-axis, respectively, i.e. the elementary one-qubit operations.

The possibility to perform the coherent manipulations described above is limited by the fact that the voltage source creating V_x and the current source creating Φ_x are inevitably noisy. The external voltage source is part of a dissipative circuit with effective resistance R_V and Johnson-Nyquist voltage fluctuations. Similarly, the circuit of the current source, with resistance R_I, which couples the flux Φ_x to the SQUID by the mutual inductance M, introduces fluctuations. Both fluctuating sources may destroy the coherence of the qubit dynamics. The corresponding parts of the qubit's Hamiltonian responsible for the coupling with the dissipative environment are in linear approximation

$$\begin{aligned} H_\mathrm{res}^V &= e\frac{C_\mathrm{qb}}{C_\mathrm{J}}\delta V_\mathrm{x}\sigma_z \\ H_\mathrm{res}^I &= \frac{\pi E_\mathrm{J}'}{\Phi_0}\sin\left(\frac{\pi\Phi_\mathrm{x}}{\Phi_0}\right) M\delta I_\mathrm{x}\sigma_x \ , \end{aligned} \tag{8}$$

where δV_x is the fluctuating part of the external voltage and δI_x is the fluctuating part of the external current which creates Φ_x. The full solution of the two level system coupled to two dissipative baths via non-commuting observables (like σ_z and σ_x in (8)) is not known. But we expect that in the weak coupling (slow decoherence) regime the effects of the two noise sources can be evaluated separately and the results add in a simple way. The dephasing effect of a single bath on a two-state quantum system has been analyzed in Refs. [16,17] and we can take over these results.

For example, in the idle state, $V_{\rm x} = V_{\rm deg}$, $\Phi_{\rm x} = \Phi_0/2$, when the qubit's Hamiltonian $H = 0$ vanishes, both noise sources are relevant. If only the flux noise were present, it would destroy the relative phase in the σ_x basis of the qubit on a time scale

$$\tau_I^{-1} = \pi^3 \frac{R_{\rm K}}{R_I} \left(\frac{E_{\rm J}' M}{\Phi_0^2}\right)^2 \frac{k_{\rm B}T}{\hbar} \,. \tag{9}$$

This dephasing is slow if the current source is coupled weakly to the qubit (small M) and its resistance is high compared to the quantum resistance $R_{\rm K} = h/e^2 \approx 26{\rm k}\Omega$. On the other hand, if only the voltage noise were present one would get the dephasing in the σ_z basis characterized by

$$\tau_V^{-1} = 8\pi \frac{R_V}{R_{\rm K}} \left(\frac{C_{\rm qb}}{C_{\rm J}}\right)^2 \frac{k_{\rm B}T}{\hbar} \,. \tag{10}$$

The resistance of the voltage source R_V should be much smaller than $R_{\rm K}$. Furthermore, a small gate capacitance $C \ll C_{\rm J}$ helps decoupling the qubit from the environment. If both noise sources are present, the dynamics might be complicated but we would still expect the time scales (9) and (10) to characterize the relaxation.

Another important regime is $V_{\rm x} = V_{\rm deg}$, $\Phi_{\rm x} = 0$, when the charging energy vanishes $E_z^i = 0$ and the Josephson energy $E_x^i = E_{\rm J}(0)$ is maximal. In this regime the fastest possible coherent oscillations of charge with the largest possible amplitude are expected. The fluctuations $\delta I_{\rm x}$ are decoupled from the qubit's dynamics ($H_{\rm res}^I = 0$) while the voltage fluctuations suppress the coherent oscillations on the time scale

$$\tau_V^{-1} = 4\pi \frac{R_V}{R_{\rm K}} \left(\frac{C_{\rm qb}}{C_{\rm J}}\right)^2 \frac{E_{\rm J}(0)}{\hbar} \coth\left(\frac{E_{\rm J}(0)}{2k_{\rm B}T}\right) \,. \tag{11}$$

Again two small ratios $R_V/R_{\rm K}$ and $C_{\rm qb}/C_{\rm J}$ help decrease the effect of the environment. Both can be optimized to provide a long phase coherence time, larger by several orders of magnitude compared to typical operation times $\hbar/E_{\rm J}(0)$ (the period of the coherent oscillations).

Inter-qubit coupling. To perform two-bit operations the qubits must be coupled. The simplest implementation of the coupling is to connect all N qubits in parallel to each other to an inductor L (Fig. 3). As a result an LC oscillator is formed in the system by the inductor L and by the total capacitance of all qubits $NC_{\rm qb}$. If the frequency of this LC-mode is large, $\hbar\omega_{LC} = \hbar(NC_{\rm qb}L)^{-1/2} \gg E_{\rm J}, E_{\rm ch}, k_{\rm B}T$, the oscillator is always found in its ground state. Nevertheless, the virtual processes which involve the excited states of the oscillator produce an effective coupling between the qubits

$$H_{\rm int} = -\sum_{i<j} \frac{E_{\rm J}^i E_{\rm J}^j}{E_L} \hat\sigma_y^i \hat\sigma_y^j. \tag{12}$$

Here $E_L = \frac{\Phi_0^2}{\pi^2 L}\left(\frac{C_{\rm J}}{C_{\rm qb}}\right)^2$, and $E_{\rm J}^i = E_{\rm J}(\Phi_{{\rm x}i})$ are the effective, flux-controlled Josephson energies of the qubits. The coupling energy (12) can be understood as the magnetic energy of the total current in the inductor $\sum_i LI_i^2/2$, which is the sum of contributions from all qubits, $I^i \propto E_{\rm J}^i \hat\sigma_y^i$. Note, that this way of coupling (via virtual excitations) differs from the coupling via a real excitation of a phonon mode employed in the case of trapped chains of ions [18].

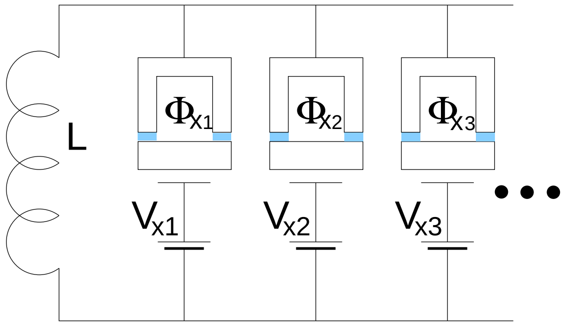

FIG. 3. **Design of a quantum computer.** The coupling of the qubits is provided by the LC-oscillator mode in circuit shown. Note that the system can be scaled to large numbers of qubits. In the idle state all effective Josephson couplings are tuned to zero and the voltages are chosen such that the charge states are degenerate. Single-bit operations are performed by changing the gate voltage or flux of one qubit at a time. Two-bit operations between any two qubits are triggered by turning on the corresponding two Josephson couplings.

With this design we can perform all gate operations. In the idle state the interaction Hamiltonian (12) is zero since all the Josephson couplings are turned off (the qubits do not contribute to the current through the inductor). The same is true during a one-qubit operation, as long as we perform one such an operation at a time: i.e. only one $E_{\rm J}^i \neq 0$. To perform a two-qubit operation with any given pair of qubits, say 1 and 2, $E_{\rm J}^1$ and $E_{\rm J}^2$ are switched on simultaneously, yielding the total Hamiltonian

$$H = -\frac{E_{\rm J}^1}{2}\hat\sigma_x^1 - \frac{E_{\rm J}^2}{2}\hat\sigma_x^2 - \frac{E_{\rm J}^1 E_{\rm J}^2}{E_L}\hat\sigma_y^1\hat\sigma_y^2 \tag{13}$$

While not identical to the form (1), also these two-bit gates, in combination with the single-bit operations discussed above, provide a complete set required for quantum computation. Indeed, even if the third term in the Hamiltonian (13) is smaller than the first two, one may use degeneracies to create entangled states. If one chooses $E_{\rm J}^1 = E_{\rm J}^2$, the states $|+_1\rangle|-_2\rangle$ and $|-_1\rangle|+_2\rangle$, where $|\pm_i\rangle \equiv 2^{-1/2}(|\downarrow_i\rangle \pm |\uparrow_i\rangle)$, are degenerate. The interaction (12) lifts this degeneracy and creates entangled states on the time scale $\hbar E_{\rm L}/(E_{\rm J}^1 E_{\rm J}^2)$. Alternatively, one can switch at the same time the charging energies so that $E_z^1 = E_z^2 \gg E_{\rm J}^1, E_{\rm J}^2$. Then the states $|\downarrow_1\rangle\,|\uparrow_2\rangle$ and $|\downarrow_2\rangle\,|\uparrow_1\rangle$ are degenerate and the interaction term (12) lifts this degeneracy as well.

To demonstrate that the constraints on the circuit parameters can be met by available technology, we suggest the following suitable set:
(i) We choose junctions with capacitance $C_{\rm J} = 400$aF, corresponding to a charging energy (in temperature units) $E_C \sim 3$K, and a smaller gate capacitance $C = 2.5$aF to reduce the coupling to the environment. The superconducting gap has to be slightly larger $\Delta > E_C$. Thus at working temperature of order $T = 50$mK the initial thermalization is assured. We further choose $E'_{\rm J} = 50$mK, i.e. the time scale of one-qubit operations is $\tau_{\rm op} = \hbar/E_{\rm J} \sim 70$ps. Fluctuations associated with the gate voltages (11), with resistance $R_V \sim 50\Omega$, limit the coherence time to $\tau_V/\tau_{\rm op} \sim 10^5 - 10^6$ one-bit operations.
(ii) If the inductance of the SQUID loop is $L_\Phi = 0.1$nH, the fluctuations of the flux are weak, $\sqrt{\langle \delta\Phi^2\rangle} \sim 0.08\Phi_0$, and, as required, the excitation energy of the Φ-degree of freedom $\hbar\omega_\Phi \sim 80$K is large compared to characteristic energy scales of the qubit. Compared to the voltage fluctuations, for reasonable values $M = 1$nH and $R_I = 10^2$–$10^6\Omega$, the flux circuit has a weak dephasing effect.
(iii) The most difficult problem appears to be the level of the two-bit coupling. For a setup in Fig. 3 one would need inductances of order of several μH. For example, if we choose the energy scale E_L of the order of $10E_{\rm J}$, we obtain $L \approx 3\mu$H. Since the energy of LC-oscillations should be large, $\hbar(NC_{\rm qb}L)^{-1/2} \gg 2E'_{\rm J},\, k_{\rm B}T$, the number of qubits in the circuit is limited by $N_{\rm max} \sim 70$. The inductance of order $L \approx 3\mu$H is quite large for a mesoscopic setup. A pure geometric inductance (a coil) is problematic due to stray capacitances. Alternatively one can build an effective inductance out of several Josephson junctions connected in sequence. The basic idea is to use the junctions in the classical ("phase") regime when the phase drop on each of them is much smaller than the flux quantum Φ_0. Then the Josephson energy $E_{\rm J}\,(1-\cos(2\pi\Phi/\Phi_0)) \approx \Phi^2/2L_{\rm J}$ where $L_{\rm J} \equiv \Phi_0^2/4\pi^2 E_{\rm J}$. Such junctions have there own capacitance and, therefore, can not be regarded as pure inductances. This, however, may be taken into account when calculating the frequency of the LC mode. Still, estimates show that one needs $10^2 - 10^3$ such junctions. The problem of the setup in Fig. 3 is in the double role played by the small ratio of the capacitances $C_{\rm qb}/C_{\rm J}$. On one hand, its smallness allows us to decouple the qubit from the electromagnetic environment and to achieve reasonably long dephasing times (see e.g. Eqs. (11,10)). On the other hand, the same smallness effectively decouples the qubits from each other (see Eq. (12)). This problem is solved by a setup as shown in Fig. 4. Here one should demand $C_{\rm V}/C_{\rm J}$ to be small in order to decouple from the electromagnetic fluctuations coming from the voltage source. As there are no dissipative elements in the inductance circuit, the ratio $C_{\rm L}/C_{\rm J}$ may be of order one. Then the charging energy of the qubit is renormalized by a factor of order one, while the inter-qubit coupling is increased significantly. Estimates show reasonable level of coupling for $L \approx 1$nH, which may be achieved with only several "classical" Josephson junctions.

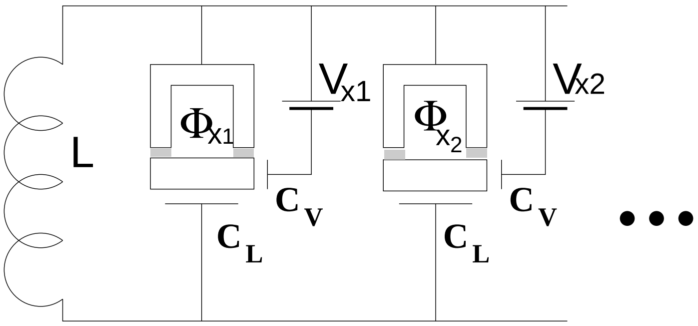

FIG. 4. **Design which allows for stronger inter-qubit couplings.** By separating the circuit of the control voltage from the circuit of the LC oscillator one achieves low dephasing and reasonable level of inter-qubit coupling.

Further remarks on the design and manipulation of the system are in order: (i) The two lowest states of the qubit are separated from higher states, which exist in the physical system, by the energies $E_C, \hbar\omega_{LC}, \hbar\omega_\Phi$. If, in addition, switching processes of $V_{\rm x}$ and $\Phi_{\rm x}$ are slow on the corresponding time scales, the requirements presented above also ensure that the higher states are not excited. Alternatively, instead of sudden switching, one change the biases adiabatically. (ii) The system presented here does not permit parallel operations on different qubits, which is employed in many powerful quantum algorithms. It can be achieved in principle by a more advanced design, making use, e.g., of further tunable SQUIDs decoupling different parts of the circuit. Such modifications, as well as further progress of nano-technology, will provide longer coherence times and allow scaling to larger numbers of qubits.

Measurement process In addition to the manipulation of qubits the resulting quantum state has to be read out [10,11]. This can be accomplished by coupling a single-electron transistor (SET) capacitively to the qubit as shown in Fig. 5. As long as no transport voltage is applied to the SET, no dissipative currents flow, and the presence of the SET merely renormalizes (weakly) the parameters of the qubit. To perform a measurement, the transport voltage is turned on. The measurement process makes use of the high sensitivity of the current through the SET (the meter) to the voltage applied to the middle island. Since different states of the qubit differ in charge, the voltage felt by the SET, and the macroscopic, measurable current through it, depend on the state of the qubit.

In order to investigate the measurement process we evaluate explicitly the time-evolution of the density matrix of the combined system. The latter can be reduced by tracing over microscopic degrees of freedom while keeping track only of N, the charge on the middle island of the SET, m, the total charge that has tunneled through the SET, and n, the charge degree of freedom of the qubit. The result is a matrix $\rho^{iN\,m}_{jN'm'}(t)$. Here $i,j = 0,1$ refer to a basis of qubit states. Performing the analysis we find that a closed set of equations can be derived for $\rho^{ij}_N(m) \equiv \rho^{iNm}_{jNm}$, i.e. the elements of the density matrix which are diagonal in N and m. We derive a master equation for the time evolution of this quantity and analyze its solutions for a given initial state of the qubit. The density matrix can be further reduced to that of the qubit, $\rho^{ij}_{(\mathrm{qb})}(t) \equiv \sum_{N,m} \rho^{ij}_N(m,t)$, and we can derive from it the probability that m electrons have passed by time t through the SET, $P(m,t) \equiv \sum_{N,j} \rho^{jj}_N(m,t)$.

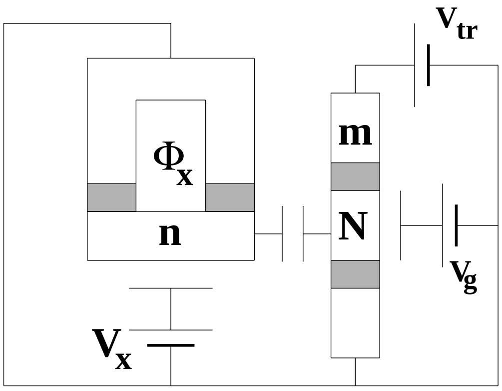

FIG. 5. The circuit consisting of a qubit plus a SET transistor used as a measuring device.

We neglect equilibrium relaxation processes (due to the fluctuations in the voltage and flux sources) assuming that all the time scales characterizing the measurement are much shorter then those characterizing the equilibrium relaxation. This assumption must be confirmed later for selfconsistency. Then, we find that the measurement process is characterized by three time scales, which have to be ordered as $t_{\mathrm{mix}} \gg t_{\mathrm{meas}} > \tau_\varphi$ in order for the measurement to be effective. Two times show up in the dynamics of the qubit's reduced density matrix, $\rho^{ij}_{\mathrm{qb}}(t)$. On the shortest scale, the dephasing time τ_φ, the phase coherence between two eigenstates of the qubit is lost, while their occupation probabilities remain unchanged. Later, measurement-induced transitions mix the eigenstates, changing their occupation probabilities on a time scale $t_{\mathrm{mix}} > \tau_\varphi$. The reason for mixing is that the charge (the measured quantity) does not commute with the qubit's Hamiltonian in the presence of the finite Josephson coupling $E_{\mathrm{J}}(\Phi_x)$. In other words, the "measurement basis" and the eigenbasis of the qubit differ. In principle, with the improved design of the qubit (Fig. 1b), we can get read of the mixing completely by making $E_{\mathrm{J}} = 0$ during the measurement. Still we discuss the mixing time since (i) there might always be some residual finite E_{J} due to imperfectness of the design (ii) making E_{J} finite deliberately one may effectively calibrate the measuring device and learn about its time scales from the stationary noise spectrum, as we will see below. The third time scale shows up in the dynamics of $P(m,t)$. Due to intrinsic noise this distribution displays a signal only after the time t_{meas}. It is longer than τ_φ. If, furthermore, $t_{\mathrm{mix}} \gg t_{\mathrm{meas}}$ the distribution $P(m,t)$ develops at times $t \geq t_{\mathrm{meas}}$ a double-peak structure with the weights of the peaks given by the initial occupation probabilities of the eigenstates. Hence the measurement of $P(m,t)$ constitutes a measurement process of the qubit's state. At longer times, on the scale t_{mix}, the structure of $P(m,t)$ is smeared by mixing and the information about the qubit's state is lost.

The system parameters required for an effective measurement and the dependence of the three time scales on these parameters were analyzed in Refs. [10,11]. Rather than discussing all possible regimes we provide a flavor of the scales involved by giving a concrete example: If the normal tunnel barriers of the SET are characterized by the capacitances of order 10aF and by tunnel resistances of order $R_{\mathrm{T}} \approx 0.25 * R_{\mathrm{K}}$ ($R_{\mathrm{K}} \equiv h/e^2 \approx 25.8k\Omega$), while all the gate capacitances (including the capacitance between the SET and the qubit) are of order 1aF, we obtain $t_{\mathrm{meas}} \approx 10^{-8} - 10^{-7}$s and $t_{\mathrm{mix}} \approx 10^{-6}$s for $E_{\mathrm{J}} = 0.1$K. The measurement time t_{meas}, in this example, is much shorter than the equilibrium relaxation times (11,9,10). Thus, one can neglect those processes during the measurement. On the other hand the mixing time t_{mix} might be close to the equilibrium relaxation times and the long time behavior of the current in the measuring device may depend on the relation between these times.

For a time we keep neglecting the equilibrium relaxation (assuming thus that t_{meas} and t_{mix} are much shorter than the times (11,9,10)) and discuss the statistics of charge and current in the measuring device at all times. The distribution $P(m,t)$ does not contain all information about the statistics, e.g. we cannot deduce from it the probability to observe a given value of current, $P(I,t)$, or the noise spectrum of the current. To analyze the statistics of the current we have to analyze also the two-time correlator $P(m_1,t_1;m_2,t_2)$, i.e. the probability that m_1 electrons have passed through the SET by time t_1 and m_2 electrons by time t_2. Knowing this correlator we can calculate various statistical characteristics of the current. One of them is the probability to observe a given value of current, averaged over a time interval Δt, at a given time t. Introduce $I_{\Delta t} \equiv [m(t+\Delta t) - m(t)]/\Delta t = \Delta m/\Delta t$ we have

$$P(I_{\Delta t}, t) \equiv \sum_m P(m + \Delta m, t + \Delta t; m, t) \ . \tag{14}$$

Another interesting characteristic is the charge-charge correlator

$$\langle m(t_1)\, m(t_2)\rangle = \sum_{m_1, m_2} m_1\, m_2\, P(m_1, t_1; m_2, t_2) \ , \tag{15}$$

from which the spectrum of noise may be calculated.

The behavior of $P(I_{\Delta t}, t)$ for different values of the time scales is presented in Fig. 6. We see that the measurement of the current constitutes a quantum measurement only in regime (b), i.e., when $t_{\rm meas} < \Delta t < t_{\rm mix}$ and $t < t_{\rm mix}$. In this case the current is approximately equal to I_0 or to I_1 with probabilities $|a|^2$ and $|b|^2$, respectively. In regime (a) the meter is too sensitive and we cannot extract the information on the background of the noise. In regime (d) the meter induces mixing before one can read out the information. Finally, in regime (c), we still observe two peaks around I_0 and I_1, but with equal probabilities. This indicates that a typical current pattern would look like a telegraph signal jumping between I_0 and I_1 every $t_{\rm mix}$ on average.

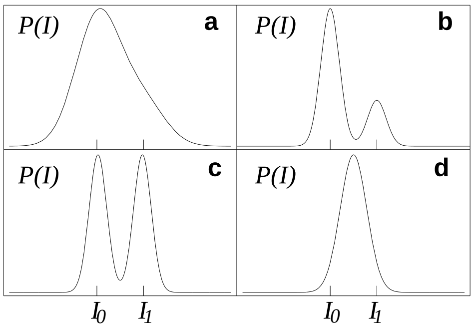

FIG. 6. The probability to observe a given value of current at a given time. It is assumed that the qubit is prepared initially in a coherent superposition of its eigenstates $a|0\rangle + b|1\rangle$ with $|a|^2 = 0.75$ and $|b|^2 = 0.25$. The time scales are chosen as follows: (a) $\Delta t < t_{\rm ms}$, any t; (b) $t_{\rm meas} < \Delta t < t_{\rm mix}$, $t < t_{\rm mix}$; (c) $t_{\rm meas} < \Delta t < t_{\rm mix}$, $t > t_{\rm mix}$; (d) $t_{\rm mix} < \Delta t, t$.

We obtain another evidence of the "telegraph" pattern of the current when analyzing the frequency dependence of the current noise in the SET. In the stationary regime $(t \gg \Gamma_{\rm mix}^{-1})$ we obtain

$$S_I(\omega) = S_{\rm shot} + \frac{S_{\rm telegraph}}{1 + (t_{\rm mix}\omega)^2} \ . \tag{16}$$

The first (ω independent) term corresponds to the shot noise, while the second term originates from the telegraph noise. The ratio of the telegraph and the shot noise amplitudes at $\omega = 0$ is

$$\frac{S_{\rm telegraph}}{S_{\rm shot}} \approx \frac{t_{\rm mix}}{t_{\rm meas}} \ , \tag{17}$$

i. e., the telegraph noise becomes noticeable above the shot noise precisely when we approach the regime of the quantum measurement. The noise spectrum in this case is shown in Fig. 7. Taking into account the typical amplitude of the 1/f noise observed in many experiments we conclude that there exists a window of frequencies where the telegraph noise is dominant.

Finally, we discuss the possible effects of the equilibrium relaxation. If the time scale of this relaxation becomes shorter than $t_{\rm mix}$ (or equivalently $t_{\rm mix}$ becomes too long), but it is still longer than the measurement time $t_{\rm meas}$, the quantum measurement can still be performed. The "telegraph" noise feature is, however, lost in this regime. Indeed, the thermal equilibration in this case is stronger than the measurement induced mixing and after a time of order (11,9,10) the qubit will be forced into a thermal state (ground state for low temperatures) even before a single jump of the "telegraph" noise has occurred. The low frequency ($\omega < t_{\rm meas}$) measurement of the current will show then only one possible value of the current (e.g. I_0 if $|0\rangle$ is the ground state) as was observed in Ref. [6]. If the times (11,9,10) are even shorter than $t_{\rm meas}$ no quantum measurement can be performed (but the measurement of the type of Ref. [6] can still be done. Thus, changing deliberately $t_{\rm mix}$ by controlling the Josephson coupling one can drive the system form the "ground state current" regime to the "telegraph" noise regime. Observation of the "telegraph" noise would put a lower bound on the equilibrium relaxation times and it would prove that the system is calibrated into the quantum measurement regime.

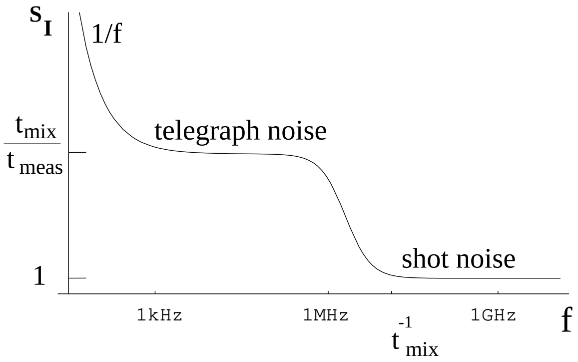

FIG. 7. Noise spectrum of the current in the SET in the stationary regime. The typical amplitude of the 1/f noise can be estimated from the available experimental data.

Thus, by analyzing the time dependence of the density matrix of the system composed of the qubit and the SET we have provided a systematic and complete description of the quantum measurement process. We have calculated the experimentally observable macroscopic quantities (the current or the number of electrons which have tunneled) fully within the framework of the time-dependent Schrödinger equation. We have shown that they contain the information about the quantum state of the qubit before the process. We did not need to invoke additional concepts like 'collapse of the wave function' [19] or extra assumptions about the knowledge of the observer [20]. Our approach extends earlier work on the 'which-path experiments' in Aharonov-Bohm structures containing a quantum dot [21–24]. In this work it was demonstrated that the current in a nearby point contact, which interacts with the dot electrons provides a measurement since it reduces the quantum interference effects. But no information was obtained for the current itself. The information contained in the current was discussed by us [10] for the practical case of a SET coupled to a Josephson qubit and, later, by several authors [19,20,25] for an idealized QPC system. In the latter $t_{\mathrm{meas}} \approx \tau_\varphi$ and in this sense it realizes a 100% efficient measurement. In contrast to this discussion of an ideal experiment, our goal has been the description of a realistic, practically used device.

To conclude, the realization of many Josephson qubits with controlled coupling and measurement devices (SET) attached is possible with current nano-scale technology. In such systems fundamental features of macroscopic quantum-mechanics and crucial steps on the way to quantum computation can be explored. Experimentally it is now well established that these system may be prepared in superpositions of charge states [6–8]. The time resolved experiments are limited by the accuracy of the time control and by the smearing effect of the external circuits. In this context the breakthrough experiment of Nakamura et al. [9] shows that these difficulties can be overcome.

---

[1] A. Shnirman, G. Schön, and Z. Hermon, Phys. Rev. Lett. **79**, 2371 (1997).
[2] Yu. Makhlin, G. Schön, and A. Shnirman, Nature **386**, 305 (1999).
[3] D.V. Averin, Solid State Commun. **105**, 659 (1998).
[4] L.B. Ioffe, V.B. Geshkenbein, M.V. Feigel'man, A.L. Fauchere, and G. Blatter, Nature **398**, 679 (1999).
[5] J.E. Mooij, T.P Orlando, L. Levitiov, Lin Tian, C. H. van der Wal, and S. Lloyd, Science **285**, 1036 (1999).
[6] V. Bouchiat, Ph. D. Thesis, Université Paris 6 (1997); V. Bouchiat, D. Vion, P. Joyez, D. Esteve, and M.H. Devoret, Physica Scripta **T76**, 165 (1998).
[7] A. Maassen van den Brink, G. Schön, and L.J. Geerligs, Phys. Rev. Lett. **67**, 3030 (1991).
[8] Y. Nakamura, C.D. Chen, and J.S. Tsai, Phys. Rev. Lett. **79**, 2328 (1997).
[9] Y. Nakamura, Yu.A. Pashkin, and J.S. Tsai, Nature **398**, 786 (1999).
[10] A. Shnirman and G. Schön, Phys. Rev. B **57**, 15400 (1998).
[11] Y. Makhlin, G. Schön, and A. Shnirman, to be published in "Exploring the Quantum-Classical Frontier: Recent Advances in Macroscopic and Mesoscopic Quantum Phenomena." Eds. J.R.Friedman and S.Han, cond-mat/9811029.
[12] Y. Makhlin, G. Schön, and A. Shnirman, submitted to Phys. Rev. Lett., cond-mat/0001423.
[13] Barenco, A. et al. Elementary gates for quantum computation. *Phys. Rev. A* **52**, 3457 (1995).
[14] M. Tinkham, *Introduction to Superconductivity*, 2nd edition, McGraw-Hill (1996).
[15] R. Rouse, S. Han, and J.E. Lukens, Phys. Rev. Lett. **75**, 1614 (1995).
[16] A.J. Leggett, S. Chakravarty, A.T. Dorsey, M.P.A. Fisher, A. Garg, and W. Zwerger, Rev. Mod. Phys. **59**, 1 (1987).
[17] U. Weiss and M. Wollensak, Phys. Rev. Lett. **62**, 1663 (1989); R. Görlich, M. Sassetti and U. Weiss, Europhys. Lett. **10**, 507 (1989).
[18] J.I. Cirac and P. Zoller, Phys. Rev. Lett. **74**, 4091 (1995).
[19] S.A. Gurvitz, preprint, quant-ph/9808058.
[20] A.N. Korotkov, Phys. Rev. B **60**, 5737 (1999).
[21] E. Buks, R. Schuster, M. Heiblum, D. Mahalu, and V. Umansky, Nature, **391**, 871 (1998).
[22] I.L. Aleiner, N.S. Wingreen, Y. Meir, Phys. Rev. Lett. **79**, 3740 (1997).
[23] Y. Levinson, Europhys. Lett. **39**, 299 (1997).
[24] S.A. Gurvitz, Phys. Rev. B **56**, 15215 (1997).
[25] L. Stodolsky, Phys. Lett. B **459**, 193 (1999).